

**A facile synthesis of a room-temperature chiral discotic nematic liquid crystal based on pentaalkynylbenzene core**

Huanan Yu,<sup>\*a</sup> Georg H Mehl<sup>b</sup>

*<sup>a</sup>School of Materials and Chemistry, China Jiliang University, Hangzhou, China*

*<sup>b</sup>Department of Chemistry, University of Hull, Hull, HU6 7RX, United Kingdom*

E-mail: yhnzzu@163.com

# **A facile synthesis of a room-temperature chiral discotic nematic liquid crystal based on pentaalkynylbenzene core**

The preparation of discotic liquid crystal with a wide thermal nematic phase range remains a challenge. Here, a method to synthesize a class of discotic liquid crystal with exclusive and stable chiral nematic phase over a wide temperature range, based on pentaalkynylbenzene core, is presented and the mesogenic properties are well studied.

Keywords: Discotic liquid crystal; chiral nematic, room-temperature, pentaalkynylbenzene core

## **1. Introduction**

Owing to the spontaneously one dimensional stacks in disk-shaped molecules caused by the driving forces of nanophase segregation and the minimization of free volume, columnar mesomorphism have dominated the field of discotic liquid crystals (DLCs) and received particular interest in charge transport [1-4]. Very few examples of DLCs exhibit a less ordered nematic phase ( $N_D$ ), which have been found commercial use as active switching components and optical compensation films to widen the viewing angle in display technologies [5, 6]. As well, most currently reported discotic nematogens show the  $N_D$  phase at high temperature and over a narrow thermal range [7]. Chiral DLCs raised significant interest since the tilted phase of chiral discotic dibenzopyrene derivatives was reported ferroelectric for the first time [8, 9]. Taing and co-workers developed a strategy to incorporate chiral branched chain into discotic nematogen [10]. However, the incorporation of chirality unexpectedly enhances the nucleation and crystal growth well above the temperature ranges of their hypothetical nematic phases. Up to now, efforts to induce the excellent chiral nematic phase ( $N_D^*$ ) behaviour of DLCs have proven limited [11]. Rare cases realized the implementation of thermally stable  $N_D^*$  phase at room temperature [12]. This makes the development of the chiral discotic nematogens highly attractive and desirable.

Pentaalkynylbenzene (PA) derivatives have been one of the most widely investigated systems for various discotic nematogens [13, 14]. In this case, the reduced stacking interactions contributed by the conformational flexible and sterically hindered cores; the phenyl rings are generally not in plane because of the rotational freedom provided by ethynyl linkers which prevents columnar stacking, together with the attachment of the alkyl side-chains which generate insufficient packing volume, favour the nematic mesomorphism in DLCs [15-17]. Besides, the orientational freedom of the PA group increases *via* increasing the terminal alkyl chain length. Thus, the chiral functionalisation of the PA core are highly expected to tailor the discotic nematogens with desirable mesomorphic and other physical properties for the use of chiral DLCs in devices.

Liquid crystalline (LC) dendrimer systems bearing optically-active mesogens provides a strategy towards realizing the  $N_D^*$  phase behaviour in discogens [18]. A conceptually related PA-chiral tail system was expected to induce the excellent  $N_D^*$  properties (Scheme 1). Here, we report the facile synthesis and full characterisation of analogous PA material modified with a chiral dithiolane function. The precursor PA derivative **5** with a hydroxyl end shows the  $N_D$  phase above 100 °C and the incorporation of the chirality *via* an esterification reaction with (R)-(+)-1,2-dithiolane-3-pentanoic acid surprisingly contributes to forming a room-temperature  $N_D^*$  phase which persists over a wide thermal range.

## 2. Experimental

### 2.1 Materials and methods

All chemicals were purchased from Sigma-Aldrich and used as received. All solvents were of AR quality and used without further purification. Column chromatographic

separations were performed on silica gel (60-120, 100-200 & 230-400 mesh). Thin layer chromatography (TLC) was performed on aluminum sheets pre-coated with silica gel (TLC Silicagel 60 F<sub>254</sub>, Merck KGaA, Germany).

The chemical structures of the synthesised compounds were determined by a combination of spectroscopic techniques. <sup>1</sup>H-NMR characterizations of intermediates and discogens were recorded at 400 MHz on a JEOL Eclipse 400 FT NMR spectrometer at ambient temperatures. Deuterated chloroform (CDCl<sub>3</sub>) was used as a solvent and tetramethylsilane was used as an internal standard. UV/Vis spectra were recorded on Lambda 25 (Perkin-Elmer). The LC properties of the synthesised compounds were investigated using polarized light optical microscopy (POM) and differential scanning calorimetry (DSC) studies. DSC data was collected on a Mettler-Toledo DSC822e in nitrogen against an indium standard. Phase assignments of the samples were carried out using an Olympus BX51 polarizing microscope. The microscope was equipped with a Mettler-Toledo FP900 heating stage. High-resolution small-angle powder diffraction experiments were recorded on Beamlines BL16B1 at Shanghai Synchrotron Radiation Facility (SSRF). Samples were held in evacuated 1 mm capillaries. A modified Linkam hot stage with a thermal stability within 0.2 °C was used, with a hole for the capillary drilled through the silver heating block and mica windows attached to it on each side. *q* calibration and linearization were verified using several orders of layer reflections from silver behemate and a series of *n*-alkanes. A Pilatus detector was used for SAXS. Synchrotron radiation circular dichroism (SRCD) spectroscopy experiments were performed at beamline B23 of the Diamond Light Source. An intense synchrotron-generated light beam of 0.8 x 1.5 mm<sup>2</sup> in diameter was used in the spectrometer, with the ability of samples to be scanned in *xy* plane and rotated. The beam was deflected vertically

through the sample held horizontally between two quartz glass windows in a Linkam hot stage.

## 2.2 Synthesis

All reactions were conducted under nitrogen. The precursor PA derivative **5** with a hydroxyl end was synthesized by a referenced method (see the details in Supporting Information). For the preparation of the target chiral discogen **6**, precursor discogen **5** (100.0 mg, 0.09 mmol), (R)-(+)-1, 2-Dithiolane-3-pentanoic acid (65.0 mg, 0.32 mmol) and DMAP (37.0 mg, 0.30 mmol) were dissolved in dry DCM (15 ml). The mixture was deoxygenated with bubbling nitrogen for 1 hour. Then DIC (0.16 ml, 1.00 mmol) was added in one portion and it was stirred at RT under nitrogen atmosphere for 3 days. The solvent was evaporated and the product was purified by column chromatography (hexane/ethyl acetate 4:1) to obtain the first spot on the TLC plate. After re-crystallization in hexane, yellow crystals **6** was obtained (0.11 g, 93.1%). The target chiral discogen **6** was stored in *vacuum* desiccators in the dark.

## 2.3 Preparation of homeotropic cell

The helical pitch of chiral discogen here was measured by a homeotropic cell. The test cell was purchased from Japan (KSHH-25/A107P1NSS, E.H.C., Tokyo, Japan) and the known cell gap = 25  $\mu\text{m}$  is used to calculate the helical pitch. On a heating stage with temperature higher than isotropic transition temperature of chiral discogen (105  $^{\circ}\text{C}$ ), the cell gap was filled with material by capillary force and the cell was left for another 2 hours before Polarized light optical microscopy (POM) observation. Besides, the homeotropic cell method was also used to calculate the helical twist power (HTP) of chiral discogen in hydroxyl-end achiral discogen. Mixture of 50 mol% chiral discogen in host matrix was dissolved in dichloromethane by stirring. Thereafter, the solvent was

completely evaporated in an oven at 70 °C overnight. On a heating stage with temperature higher than the isotropic transition temperature of host LC (180 °C), the cell gap was filled with mixture by capillary force and the cell was left for another 2 hours before POM observation.

### **3. Results and discussion**

#### ***3.1 Synthetic route of chiral discogen 6***

Control of the mesogenic properties is an important factor in the structural design. Essentially, the attachment of laterally linked flexible alkyl side-chains **3** (Scheme S1) was used to promote the desired N<sub>D</sub> phase behaviour. Indeed, the discogen **5** exhibits exclusively the nematic phase. The inclusion of hydroxyl moiety within the flexible spacer would provide convenient access to target compound **6**. The target compound **6** was synthesized by the route depicted in Scheme 1. The synthesis of intermediates **1-5** have been reported before [19, 20]. Compound **6** was prepared conveniently by one step and the simple esterification reaction between precursor discogen **5** and (R)-(+)-1, 2-dithiolane-3-pentanoic acid led to a high yield of compound **6** up to 93.1%. All compounds were characterized by <sup>1</sup>H-NMR and Mass Spectrometry (MS) (Figure S1-8). Note the dithiolanes here or lipoic acid, have been regularly used for the attachment to gold and other metal surfaces as dithiolates [21]. The group is also known to polymerize somewhat easily. Thus the target chiral discogen **6** was stored in a *vacuum* desiccator in the dark.

#### ***3.2 Mesophase behavior of chiral discogen 6***

Thermal transitions and phase assignments were characterized by differential scanning calorimetry (DSC) together with polarized light optical microscopy (POM). Compound **5** was light-yellow crystals at room temperature and it displayed a melting transition at

104 °C to mesophase (Figure S9). Upon further heating, the mesophase was cleared at 152 °C with a transition heat ( $\Delta H$ ) of 0.61 kJ/mol. On cooling, the appearance of a well-defined *schlieren* texture (Figure S10) happened at 151 °C and it remained stable down to 83 °C. POM and DSC investigations on compound **6** confirmed a thermodynamically stable (enantiotropic) chiral nematic phase. In Figure 1, the observed POM texture at 75 °C was characteristic oily streaks, similar to the appearance of chiral nematic phase ( $N^*$ ) formed by rod-shaped mesogens [22]. By changing the polarizer angles from 0° to 110°, the reflective colour in texture went through orange, blue, grayish green and yellow, successively because of the helically twisted LC structure. The DSC traces obtained from heating and cooling runs for chiral discogen was shown in Figure 2. On heating, a  $N_D^*$  phase was observed at 49 °C, preceded by a crystal-crystal transition at lower temperature, and it turned into an isotropic liquid at 95 °C ( $\Delta H = 0.20$  kJ/mol). Formation of the  $N_D^*$  phase from isotropic state on cooling started from 94 °C with a transition enthalpy of 0.12 kJ/mol, followed by a slow crystallisation occurring at a low temperature of 5 °C. These low transition enthalpies for discogen **5** and chiral discogen **6** are consistent with the formation of the less common nematic discotic rather than columnar discotic mesophases [6]. Diffractograms of mesophases of chiral discogen **6** (Figure S11b and c) displaying a weak small angle peak with broad low intensity reflections for the lateral packing and stacking of the molecules further support the assignments as nematic DLC phase. The calculated  $d$ -spacing of around 19.97 Å for the signal in the small angle region corresponds to the separation between the PA units and thus approximates the diameter

of a single PA disk ( $\sim 19 \text{ \AA}$ ). Generally, the chiral phase behaviour of discogen **6** was exclusive and stable over a wide temperature range up to  $46 \text{ }^\circ\text{C}$ .

### 3.3 Helical pitch of chiral discogen **6**

On cooling from  $93 \text{ }^\circ\text{C}$  to  $44 \text{ }^\circ\text{C}$  in Figure S12, the helical pitch in the  $N_D^*$  phase of discogen **6** increased and the reflective colour in texture tended to change from grayish green to red. As the colour in texture varied by lowering temperature during POM observation, the question that whether the helical pitch in  $N_D^*$  phase of discogen **6** reflect the visible light selectively remained. To explore this question, we recorded synchrotron radiation circular dichroism (SRCD) spectra of discogen **6** as a function of temperature (Figure S13). Above the isotropic temperature, the CD signals around  $235 \text{ nm}$ ,  $270 \text{ nm}$ ,  $380 \text{ nm}$  and  $425 \text{ nm}$  correspond to the characteristic UV-Vis absorption (Figure S15b). The Cotton effect is positive because the optical rotation first increases as the wavelength decreases in the vicinity of absorption band for chiral discogen. The largest jump (the largest increase in ellipticity) at  $467 \text{ nm}$  is seen between  $95$  and  $100 \text{ }^\circ\text{C}$ , i.e. at the isotropic-mesophase transition temperature, coinciding with the transition temperature observed by DSC in Figure 2. The CD band outside the chromophoric absorption region is resulted from the scattering effects [23]. It should be noted that the CD band close to  $467 \text{ nm}$  did not increase by lowering temperature. Thus, the helical structure did not reflect visible light selectively and the wavelength of reflection band is not related to helical pitch by the relation  $\lambda = np$ , where  $n$  is the average refractive index of chiral discogen. When the chiral discogen was prepared in a homeotropic cell (Figure S14), bundles of well-defined lines were observed. This can be used to evaluate the helical pitch in the chiral discogen. In such a homeotropic anchoring cell, the long molecular axis is generally inclined relative to the glass plates and the chiral helical axis is parallel to the bounding substrate. These lines are interpreted by assigning the chiral LC phase a virtual



layer and often the layer thickness is equal to the half of helical pitch. The pitch in the helical LC structure, estimated from twice the distance between adjacent lines [24], is 5.7  $\mu\text{m}$ , indicating a long helical pitch in discogen **6** outside the visible spectrum. Consequently, the changed colours on cooling during the POM observation of chiral discogen cannot be related to the selective reflection phenomena.

### ***3.4 UV-Vis studies of discogens***

Both compounds **5** and **6** showed the blue fluorescence under the long wavelength of UV lamp (365 nm) in dichloromethane (Figure S15-17) because the  $\pi$ -conjugated structure in discotic molecules has a strong ultraviolet absorption. In Figure S15a, the characteristic absorption of discogen **5** exhibits the maxima centered at 238, 261 and 351 nm with two shoulder peaks at 378 and 421 nm, a consequence of the multialkynyl benzene core. For target discogen **6**, a minor blue shift of representative absorption bands appears at 233, 259 and 348 nm with two shoulder peaks around 378 and 420 nm. The decrease of the UV-Vis peaks for discogen **6** can be attributed to the promoted molecular motion from the flexible pentanoic tail, evidenced by the promoted mesophase behaviour of compound **6** as expected in Table S1.

### ***3.5 Contact measurements of discogen 6 and other LCs***

A contact experiment between precursor discogen **5** and target chiral discogen **6** was conducted to study the influence of branching and chirality in detail. The materials were placed between two glass substrates that allowed them to mix in isotropic state freely. Figure 3a shows a POM image of the contact zone between the  $N_D$  phase of compound **5** and the isotropic liquid of **6**. The flow of discogen **6** (as an isotropic liquid) into the nematic material **5** forms a fingerprint-like texture in Figure 3b. Further cooling lead to the co-existence of fingerprint-like texture and the  $N_D^*$  phase area of the pure mesogen

**6**. Crystallization of **5** occurs at lower temperatures. During the whole cooling process, no discernable phase boundary was observed.

The mixing behaviour of chiral discogen **6** with a well-studied rod-shaped mesogen **R1** in previous work was further explored here [25]. As a reference experiment, a contact sample between disk-shaped **6** and **R1** was made as above (Figure S18). Under POM observation, the contact sample on cooling exhibits the formation of individual characteristic mesophase of pure materials, leaving an isotropic mixing region in the middle of the sample. Further cooling result in the shift of the two mesophase interfaces towards each other, indicating the solubility of one material in the other to a certain extent. The mixture did not show linear mixing behaviour at room temperature in Figure S18c, but rather showed a minimum in the clearing temperature at intermediate concentrations [26]. At 24 °C, a dark gap (an isotropic area) is seen in the middle of the photograph and the interfaces meet and slowly mix characterized by some colourful ordered lines, which can be attributed to the induced chiral mesophase in the **R1**. Based on the assumption of a linear concentration gradient, a phase diagram of the mixture can be sketched, as shown in Figure S19. It should be noted here that the phase diagram is interpreted qualitatively only. The gap in the intermediate concentrations (x-axis) means the two compounds are immiscible.

### ***3.6 Helical twisting power of chiral discogen 6 in host LCs***

The helical twisting power HTP ( $\beta_M$ , a measure for the ability of a chiral dopant to twist a nematic LC) of discogen **6** was determined in a homeotropic cell by mixing **6** with two different nematic LC hosts, rod-shaped 5CB and disk-shaped **5** [27]. Discogen **5** and **6** are completely miscible. In Figure 4, a typical fingerprint texture of the chiral nematic phase was obtained and the pitch of the helical structure can be estimated from twice the distance between two adjacent lines, due to the identity period of  $L = P/2$  [24]. The helical

pitch for 50 mol% of **6** in **5** at 110 °C is 33.04  $\mu\text{m}$ . The calculated HTP value of **6** is 0.06  $\mu\text{m}^{-1}$ . Patterns in Figure S20 show a diverging cholesteric pitch under homeotropic anchoring condition. In the strongly distorted director configuration, the dark areas represent a pseudo-isotropic homeotropically aligned nematic phase. The helical pitch for 5CB doped with 1 mol% of **6** is 57.18  $\mu\text{m}$ . The HTP value of **6** in 5CB is 1.75  $\mu\text{m}^{-1}$ . Phase separation occurred when the dopant concentrations is higher than 1 mol% of **6** in 5CB. The different HTP values of chiral discogen **6** in two host systems indicate that there is a much stronger interaction between **6** and calamitic host 5CB than discotic host **5**, because of the more complicated chemical structure of discogen host (the molecular diameter is much larger than its thickness and overall). The rod-like 5CB host with lower molecular weight allows the chirality to transfer more easily and efficiently in spite of the poor miscibility with chiral discogen **6**.

#### **4. Conclusions**

In summary, a class of chiral discogen based on pentaalkynylbenzene core is prepared and the LC properties are well studied. The presented synthesis of pentaalkynylbenzene ester is a fast and versatile method to yield target product effectively. The integration of chiral dithiolane tail with precursor discogen results in the excellent  $N_D^*$  phase behaviour of chiral discogen, which is depicted as exclusive and stable over a wide temperature range. This simple and potentially universal design on DLCs will provide a new way towards the development of new anisotropic soft materials for their usability in devices.

#### **Acknowledgements**

H.Y. thanks the China Scholarship Council (CSC) for a doctoral scholarship. We also thank Dr G. Siligardi, Dr R. Hussain and Dr T. Jávorfí for the beamline test at B23 Diamond Light Source.

## Disclosure statement

No potential conflict of interest was reported by the authors.

## References

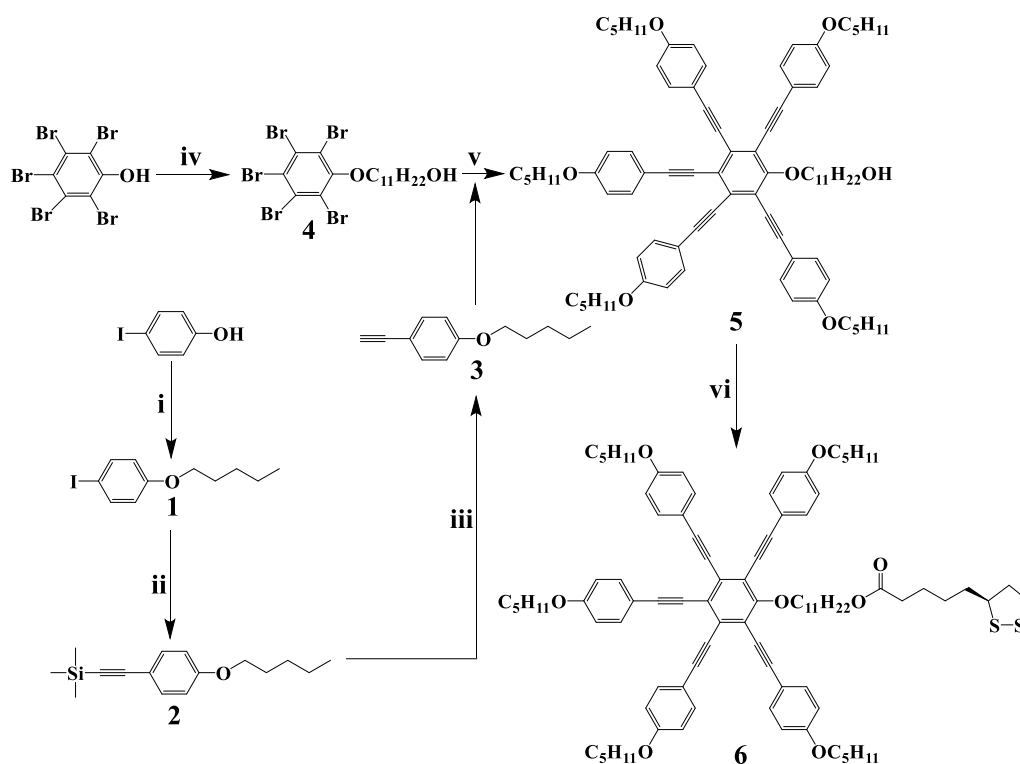
- [1] Kato T, Yoshio M, Ichikawa T, Soberats B, Ohno H, Funahashi M. Transport of ions and electrons in nanostructured liquid crystals. *Nat Rev Mater.* 2017;2:1-20.
- [2] Concellón A, Schenning APHJ, Romero P, Marcos M, Serrano JL. Size-selective adsorption in nanoporous polymers from coumarin photo-cross-linked columnar liquid crystals. *Macromolecules.* 2018;51:2349-2358.
- [3] Adam D, Schuhmacher P, Simmerer J, Häussling L, Siemensmeyer K, Etzbach KH, Ringsdorf H, Haarer D. Fast photoconduction in the highly ordered columnar phase of a discotic liquid crystal. *Nature.* 1994;371:141-143.
- [4] Kumar S. Investigations on discotic liquid crystals. *Liq Cryst.* 2020;47:1195-1203.
- [5] Feng X, Sosa-Vargas L, Umadevi S, Mori T, Shimizu Y, Hegmann T. Discotic liquid crystal-functionalized gold nanorods: 2- and 3D self-assembly and macroscopic alignment as well as increased charge carrier mobility in hexagonal columnar liquid crystal hosts affected by molecular packing and  $\pi$ - $\pi$  interactions. *Adv Funct Mater.* 2015;25:1180-1192.
- [6] Lemaire V, Filho D, Coropceanu V, Lehmann M, Geerts Y, Piris J, Debije MG, van de Craats AM, Senthilkumar K, Siebbeles LDA, Warman JM, Brédas J, Cornil J. Charge transport properties in discotic liquid crystals: a quantum-chemical insight into structure-property relationships. *J Am Chem Soc.* 2004;126:3271-3279.
- [7] Bisoyi HK, Kumar S. Discotic nematic liquid crystals: science and technology. *Chem Soc Rev.* 2010;39:264-285.
- [8] Bock H, Helfrich W. Ferroelectrically switchable columnar liquid crystal. *Liq Cryst.* 1992;12:697-703.
- [9] Spiess HW. Improving organisation of discotics: annealing, shape, side groups, chirality. *Liq Cryst.* 2020;47:1880-1885.
- [10] Taing H, Rothera JG, Binder JF, Macdonald CLB, Eichhorn SH. 1, 3, 5-Triazine (trithiophenylcarboxylate) esters form metastable monotropic nematic discotic liquid crystal phases. *Liq Cryst.* 2018;45:1147-1154.
- [11] Wöhrle T, Wurzbach I, Kirres J, Kostidou A, Kapernaum N, Littscheidt J, Haenle JC, Staffeld P, Baro A, Giesselmann F, Laschat S. Discotic liquid crystals. *Chem*

Rev. 2016;116:1139-1241.

- [12] Gupta M, Pal SK. The first examples of room temperature liquid crystal dimers based on cholesterol and pentaalkynylbenzene. *Liq Cryst.* 2015;42:1250-1256.
- [13] Ebert M, Jungbauer DA, Kleppinger R, Wendorff JH, Kohne B, Praefcke K. Structural and dynamic properties of a new type of discotic nematic compounds. *Liq Cryst.* 1989;4:53-67.
- [14] Kumar S, Varshney SK. A room-temperature discotic nematic liquid crystal, *Angew Chem Int Ed.* 2000;39:3140-3142.
- [15] Janietz D. Structure formation control of disc-shaped molecules. *Mol Cryst Liq Cryst.* 2003;396:251-264.
- [16] Gupta M, Pal SK. Structure-property relationships in lath-shaped triads based on multialkynylbenzene. *Liq Cryst.* 2018;45:1279-1286.
- [17] Gupta M, Bala I, Pal SK. A room temperature discotic mesogenic dyad based-on triphenylene and pentaalkynylbenzene. *Tetrahedron Lett.* 2014;55:5836-5840.
- [18] Frein S, Boudon J, Vonlanthen M, Scharf T, Barberád J, Süß-Fink G, Bürgi T, Deschenaux R. Liquid-crystalline thiol-and disulfide-based dendrimers for the functionalization of gold nanoparticles. *Helv Chim Acta.* 2008;91:2321-2337.
- [19] Gupta M, Mohapatra SS, Dhara S, Pal SK. Supramolecular self-assembly of thiol functionalized pentaalkynylbenzene-decorated gold nanoparticles exhibiting a room temperature discotic nematic liquid crystal phase. *J Mater Chem C.* 2018;6:2303-2310.
- [20] Apreutesei D, Mehl GH. Completely miscible disc and rod shaped molecules in the nematic phase. *Chem Commun.* 2006;6:609-611.
- [21] Turcu I, Zarafu I, Popa M, Chifiriuc MC, Bleotu C, Culita D, Ghica C, Ionita P. Lipoic acid gold nanoparticles functionalized with organic compounds as bioactive materials. *Nanomaterials.* 2017;7:43.
- [22] Held GA, Kosbar LL, Dierking I, Lowe AC, Grinstein G, Lee V, Miller RD. Confocal microscopy study of texture transitions in a polymer stabilized cholesteric liquid crystal. *Phys Rev Lett.* 1997;79:3443.
- [23] Gottarelli G, Lena S, Masiero S, Pieraccini S, Spada GP. The use of circular dichroism spectroscopy for studying the chiral molecular self-assembly: an overview. *Chirality.* 2008;20:471-485.
- [24] Dierking I. Textures of liquid crystals. John Wiley & Sons. 2003.
- [25] Cseh L, Mehl GH. The design and investigation of room temperature thermotropic

nematic gold nanoparticles. *J Am Chem Soc.* 2006;128:13376-13377.

- [26] Kouwer PHJ, Welch CJ, McRobbie G, Dodds BJ, Priest L, Mehl GH. Mixtures of disc-shaped and rod-shaped mesogens with chiral components. *J Mater Chem.* 2004;14:1798-1803.
- [27] Schreivogel A, Dawin U, Baro A, Giesselmann F, Laschat S. Chiral tetraphenylethenes as novel dopants for calamitic and discotic liquid crystals. *J Phys Org Chem.* 2009;22:484-494.



**Scheme 1.** Synthetic route of chiral discogen **6** ( $N_D^*$ ). (i) 1-Bromopentane/ $K_2CO_3$ /Butanone/ $95\text{ }^\circ\text{C}$ , (ii) TMSA/ $CuI/NEt_3/Pd(PPh_3)_2Cl_2/RT$ , (iii)  $KF/DMF/H_2O/RT$ , (iv) 11-Bromo-1-undecanol/ $K_2CO_3$ /Butanone/ $N_2/95\text{ }^\circ\text{C}$ , (v)  $PPh_3/NEt_3/Pd(PPh_3)_2Cl_2/LiBr/CuI/THF/N_2/102\text{ }^\circ\text{C}$ , (vi) (R)-(+)-1, 2-Dithiolane-3-pentanoic acid/DMAP/DIC/DCM/ $N_2/RT$ .

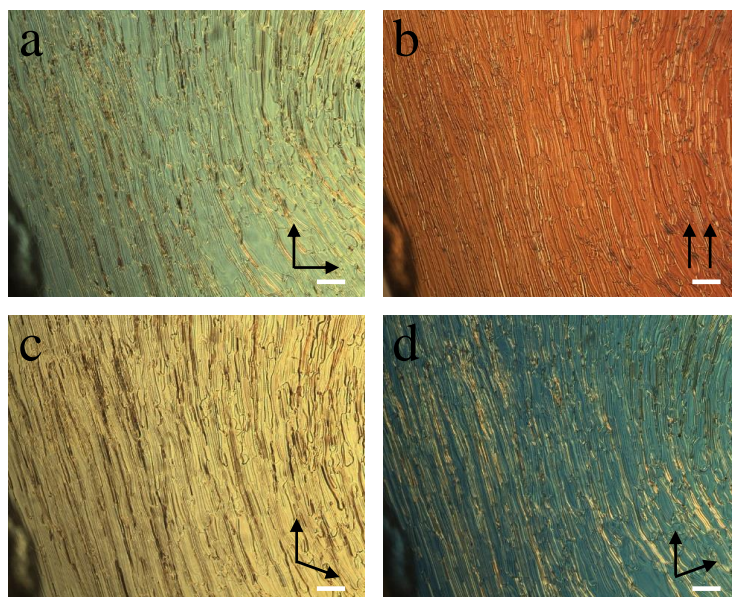


**Figure 1.** Polarized light optical microscopy (POM) micrographs(x 50  $\mu\text{m}$ ) of chiral discogen **6** ( $N_D^*$ ) (a) 75  $^\circ\text{C}$  ( $90^\circ$  crossed polarizer), (b) 75  $^\circ\text{C}$  ( $0^\circ$  crossed polarizer), (c) 75  $^\circ\text{C}$  ( $110^\circ$  crossed polarizer), (d) 75  $^\circ\text{C}$  ( $70^\circ$  crossed polarizer).



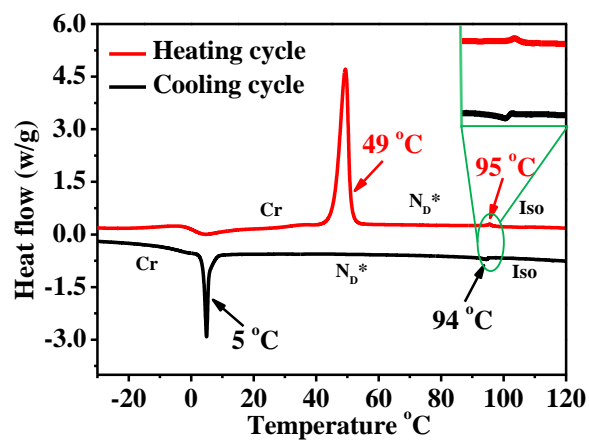


**Figure 2.** Differential scanning calorimeter (DSC) results of compound **6** at heating and cooling rate of 10 °C /min.

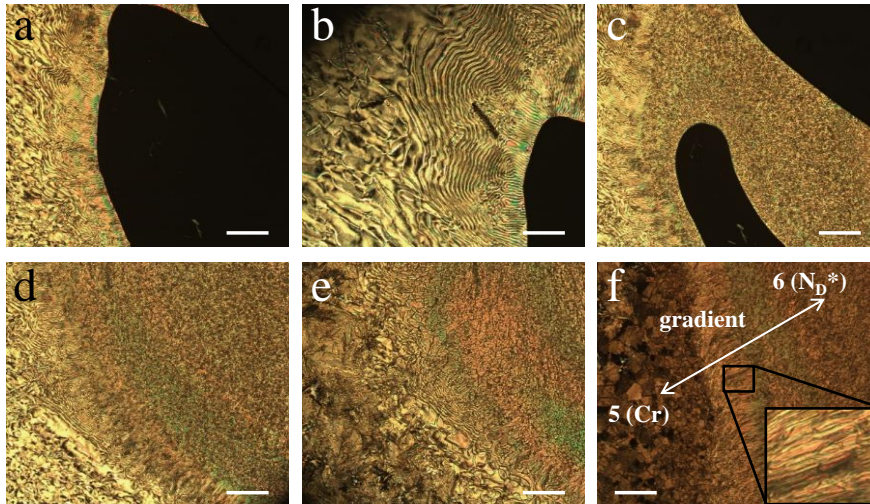


**Figure 3.** POM micrographs ( $90^\circ$  crossed polarizer) of a contact experiment for **5** (left) and **6** (right) between untreated glass slides (a)  $128^\circ\text{C}$  (x  $200\ \mu\text{m}$ ), (b)  $128^\circ\text{C}$  (x  $100\ \mu\text{m}$ ), (c)  $113^\circ\text{C}$  (x  $200\ \mu\text{m}$ ), (d)  $94^\circ\text{C}$  (x  $200\ \mu\text{m}$ ), (e)  $85^\circ\text{C}$  (x  $200\ \mu\text{m}$ ), (f)  $47^\circ\text{C}$  (x  $200\ \mu\text{m}$ ).

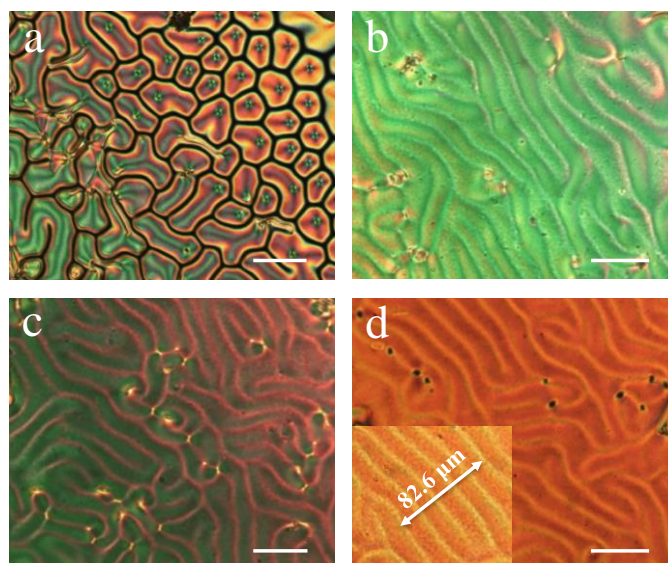


**Figure 4** POM micrographs (90° crossed polarizer) (x 50 μm) of induced  $N_D^*$  phase of **5** doped with 50 mol% of **6** in a homeotropic cell (a) 75 °C, (b) 95 °C, (c) 105 °C, (d) 110 °C.